Grid Free Lagrangian Blobs Vortex Method with Brinkman Layer Domain Embedding Approach for Heterogeneous Unsteady Thermo Fluid Dynamics Problems

Carmine GOLIA   carmine.golia@unina2.it
Faculty of Engineering, Department of
Aerospace and Mechanical Engineering
Second University of Naples
Via Roma 29, Aversa, 81031 Italy

Bernardo BUONOMO   bernardo.buonomo@unina2.it
Faculty of Engineering, Department of
Aerospace and Mechanical Engineering
Second University of Naples
Via Roma 29, Aversa, 81031 Italy

Antonio VIVIANI   antonio.viviani@unina2.it
Faculty of Engineering, Department of
Aerospace and Mechanical Engineering
Second University of Naples
Via Roma 29, Aversa, 81031 Italy

Abstract

Modeling unsteady thermal–viscous flows inside/around complicated geometries containing multiphase sub-systems (fluid–porous–solid) and multi-physics phenomena (diffusion; forced/free/mixed convection; time variations of velocity, temperatures and heat fluxes sources; still and moving bodies) is an ambitious challenge in many applications of interest in science and engineering. Scope of this exploratory work is to investigate if the combination of a grid free Lagrangian Blob method with a Brinkman layer domain embedding approach can be useful for the preliminary analysis of heterogeneous unsteady thermal buoyant problems, where easiness, readiness, short computational times, good qualitative and sufficient quantitative accuracy are the most important aspects. In this work we couple a grid free unsteady Lagrangian Thermal-Vortex Blob method with a double penalization method that considers solid bodies contoured by a fictitious buffer thin boundary layer, described by a porous Brinkman model. The model problem in this study is the interaction of a thermal buoyant plume with a solid body, still or in motion. Both solid body and Brinkman boundary layer are described by volume penalization applied by an unsteady mask method. After a description of this novel approach, preliminary analyses for validations are presented for various thermal buoyant steady/unsteady problems relative to thermal and thermal-vortical patches, fixed, free and in presence of a still or moving body. Comments on pros, contras and further work, conclude the paper.

Keywords: Buoyant Plume/Body Interaction, Lagrangian Methods, Thermal/Vortex Blobs, Grid Free, Volume Penalization, Brinkman Domain Embedding

1. INTRODUCTION

The Brinkman domain embedding approach introduces a penalty term [treated as a continuous] directly in the set of global equations over the whole flow domain, this term takes different order of magnitudes according to the particular sub domain. This approach makes the viscous body analysis almost independent on the grid domain, coordinate system, since it allows the analysis of heterogeneous problems with quite complicated geometries by using simple mask functions, and it can be used almost independently on the solution method used (FEM, FDM, Spectral method, etc.).

The advantages of this formulation are:
• Single (Cartesian or other) mesh approach to the global field, avoiding body-fitted unstructured mesh,
• Physical description of the sub domain (shape, position, size, dynamic and diffusive parameters) by simple mask functions [that can be still or can move according to the dynamics of the body].
• The warranted continuity of the diffusive fluxes across the interfaces implicitly embedded in the global equation. This automatically takes account of conjugated heat transfer problems and of coupling problems among heterogeneous media.
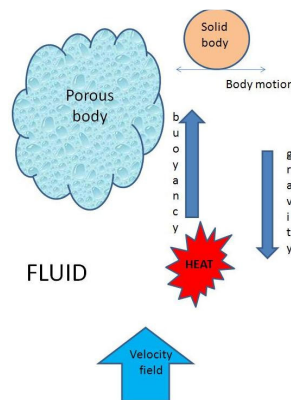

FIGURE 1: Embedding Domains.

This approach, proposed by Arquis & Caltagirone [1] and validated in Ref.s [2], [3], [4], [5], was widely used as penalization techniques for the simulation of flow around solid bodies in the contest of grid dependant computation methods, i.e. adaptive wavelet method by Schneider *et al.* ([6], [7], [8], [9], [10]); hybrid wavelet method by Vasilyev and Kevlahan [11], Kevlahan *et al.* [12]; spectral methods by Kevlahan and Ghidaglia [13].

The method has also been successfully used to simulate transitional and turbulent flows by an array of cylinders using Cartesian grids by Bruneau and Mortazavi [14] and extended to compressible flows by Chiavassa and Donat [15].

2. PRELIMINARIES

The physical idea of the penalization technique is to model the obstacle as a porous medium with porosity tending to zero. This corresponds to a Brinkman-type model with a permeability that varies according to the space domain. We can consider the whole field, treated as a global Brinkman porous medium, with properties locally varying according to the particular body treated as a specific porous media. The Navier-Stokes system is modified by adding a supplementary

term with the idea of forcing the velocity to satisfy the no-slip condition on the boundary of the obstacle. The new system is then solved in an obstacle–free computational domain.

Momentum (Navier-Stokes):

$$\frac{\partial \underline{V}}{\partial t} + \underline{V} \bullet \nabla \underline{V} = -\nabla p + \frac{1}{Re} \nabla \bullet \left[\mu \left(\nabla \underline{V} + \nabla \underline{V}^t \right) \right] - \left[\frac{\mu \left(\underline{V} - \underline{V}_{body} \right)}{Re\, Da\, K} \right] + \frac{1}{\rho_{rif}} \left(\Delta \rho \right)_T \underline{g} + \underline{f} \tag{1}$$

The value of the local specific permeability, K, models the specific embedded medium, i.e.:

$$K\left(t,\underline{r}\right) = \begin{cases} K_f & \to +\infty & \text{if } \underline{r} \in \text{fluid region} \\ K_p & & \text{if } \underline{r} \in \text{porous region} \\ K_s & \to 0^+ & \text{if } \underline{r} \in \text{solid region} \end{cases} \tag{2}$$

- In case of fluid, the "Darcy drag"is negligible with respect to the other terms and (1) reduces to the classical Navier Stokes equation.
- In case of solid, we consider a medium with porosity almost unitary and permeability nearly zero.
- In case of porous region, the "Darcy drag" term takes the role of a penalty term that imposes low velocity, so that the convective terms become negligible and (1) reduces to the classical Brinkman equation used in porous media theory:

$$\nabla p - \frac{1}{Re} \nabla \bullet \left[\mu \left(\nabla \underline{V} + \nabla \underline{V}^t \right) \right] + \left[\frac{\mu \left(\underline{V} \right)}{Re\, Da\, K_p} \right] = \frac{1}{\rho_o} \left(\Delta \rho \right)_T \underline{g} + \underline{f} \tag{3}$$

Note that the prolongation of the flow parameters [pressure, velocity and temperature inside the solid media] makes the continuity conditions on the velocity and temperature field and diffusive fluxes satisfied on and across the boundaries.

Problems may arise from the fact that in the regions where penalization constraints are imposed, the formulation is first order [as in all penalizations] and the equations become very stiff to integrate in time.

2.1 Brinkman double penalization method

Angot *et al.* [3] first proposed a "double penalization method" where a solid body is bounded by a porous Brinkman layer. This approach was used by Bruneau and Mortazavi [16, 17] to compute the viscous flow around a ground vehicle surrounded by a thin layer of porous material. Carbou [18], [19] explained the good performances of this method characterizing the boundary layer that appears over the obstacle, and in [20] by using a BKW method performed an asymptotic expansion of the solution when a little parameter, measuring the thickness of the thin layer and the inverse of the penalization coefficient, tending to zero, proved that the method is equivalent to the computations using greater thickness model by a standard Brinkman Model

2.2 Lagrangian Blob Method

The blob concept [21] is based on an attempt to make discrete the free space Dirac representation of a generic function " f " at the location (x) and time (t):

$$f\left(\underline{x},t\right) = \int f\left(\underline{x}',t\right) \delta\left(\underline{x} - \underline{x}'\right) d\underline{x}' \tag{4}$$

This representation can be made discrete, in an Eulerian formulation, as follows:

$$f\left(\underline{x}_p,t\right) = \int\limits_{\mathcal{V}} f\left(\underline{x}_q,t\right)\; W\left(\frac{\underline{x}_p - \underline{x}_q}{h}, h \right) d\mathcal{V} \tag{5}$$

where the kernel function W($\underline{r}$, h) satisfies given properties in order that, in the limit h→0, the two representations must coincide (h can be regarded as the grid size).
The Lagrangian Blob formulation is aimed to represent the value of the given field function " f " for the p-th particle that at time (t) is located in the position (x_p). This requires further modifications of eq. (5) by considering, for a finite number of particle within a cluster around the pth-particle, the following definition:

$$f\left(\underline{x}_p,t\right) = \sum_{\substack{q \in \text{Cluster} \\ \text{around} p}} f\left(\underline{x}_q,t\right) \; W\left(\frac{x_p - x_q}{h},h\right) \Delta Vol_q \qquad (6)$$

where ΔVol_q is the finite elementary volume associated with the q-th particle.
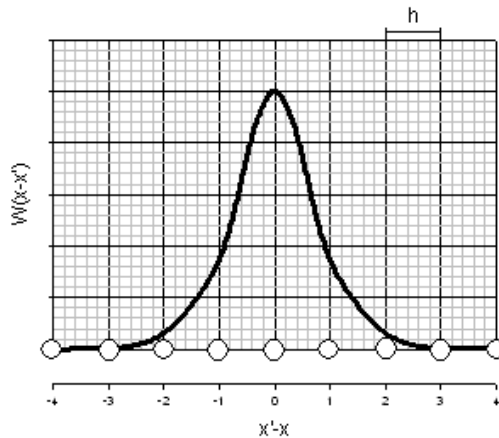

FIGURE 2: Kernel Function for the Blob Representation.

It is easy to observe that the approximations deriving from the Lagrangian Blob formulation depends on three facts:
1. The choice of the kernel function W(r, h) that must be rapidly decay with r (either Gaussian like or a polynomials compact over x/r usually equal to 1-2),
2. The computation of the integral in eq. (5) (approximated by a simple summation),
3. The finite number of particles considered in the cluster (depending on the cluster's radius).
It must be pointed out that:
• in order to allow a suitable overlap of the volumes associated to adjoining blobs a further "mollification" is performed as:

$$f_p\left(\underline{r}_p,t\right) = \sum_{\substack{q \in \text{Cluster} \\ \text{around } p}} f_q\left(\underline{r}_q,t\right) W\left(\frac{r_p - r_q}{\sigma},h\right) \Delta Vol_q \qquad (7)$$

where " $\sigma = h\,\gamma$ " is defined as the blob's radius and "γ " is an overlap parameter (usually of the order of 1 – 1.5).
• In order to be dimensionally consistent the kernel function W(r, h) must have the dimension of the inverse of a Volume (according to the dimension "d" of the space considered). Since it is usual to consider as kernels non-dimensional functions rapidly decaying, the "mollification" takes the form:

$$f_p\left(\underline{r}_p,t\right) = \sum_{\substack{q \in \text{Cluster} \\ \text{around } p}} \frac{1}{\sigma^d} W\left(\frac{r_p - r_q}{\sigma}, h\right) \left\{f_q\left(\underline{r}_q,t\right)\Delta Vol_q\right\} = \sum_{\substack{q \in \text{Cluster} \\ \text{around } p}} \frac{1}{\sigma^d} W\left(\frac{r_p - r_q}{\sigma}, h\right) F_q\left(\underline{r}_q,t\right) \qquad (8)$$

where $F_q(r_q,t) = f_q \Delta Vol_p$ is considered as the "field intensity" of the variable "f_q" over the finite volume ΔV_p.

Note that the blob representation is defined as a space average (i.e. it is an implicit sub-scale model), that is: the Lagrangian blob method for the Helmholtz formulation of the complete Navier-Stokes equations, under the limit of validity of the Boussinesq approximation, represents the space averaged equivalent equations:

$$\begin{cases} \dfrac{\partial \overline{\omega}}{\partial t} + \underline{\nabla} \bullet \left(\overline{\underline{V}\,\omega}\right) = \underline{\nabla} \bullet \left(\overline{\omega\,\underline{V}}\right) + \nu\,\nabla^2\overline{\omega} - \beta\left[\underline{g} \bullet \underline{\nabla}\overline{T}\right] \\[3mm] \dfrac{\partial \overline{T}}{\partial t} + \underline{\nabla} \bullet \left(\overline{\underline{V}\,T}\right) = \alpha\,\nabla^2\overline{T} \end{cases} \qquad (9)$$

So that, if the "h" parameter and the time integration step are small enough with respect to turbulent scale, the Lagrangian Blob method does not need any turbulent stress term, and it can be considered to represent a DNS method.

The Blob particles representation is linked to important Lagrangian conservation properties. For a general advection problem Lu=g , the blob representation satisfy the "self-adjoint-ness" condition:

$$\int_0^T \Big\langle Lu\,(\bullet,t)\,, W\left(\bullet,t\right)\Big\rangle\,dt = \Big\langle u\,(\bullet,0)\,, L*W\left(\bullet,0\right)\Big\rangle + \int_0^T \Big\langle g(t)\,, L*W\left(\bullet,t\right)\Big\rangle\,dt \qquad (10)$$

where $\langle Lu, W\rangle$ is the (space averaged) blob representation of the operator Lu, with L* its adjoint.

Obviously the Lagrangian Blob formulation of a differential problem needs the representation of all the differential operators in the problems, namely divergence, gradient and Laplacian. This may be a problem that is solved in various manners, as it will be reported later.

In conclusion Blob methods represent exact weak solution for any admissible test function (local averaged equation), i.e blob particle method achieve some (implicit) sub-grid scale model. Blobs are "Dirac particles" that directly translate with flow and transport extensive properties. They move according to velocity field, and exchange momentum and energy with neighborhood blob particles according to diffusive processes.

Blob methods then differ from classical grid techniques since they do not involve projection of the equation in a finite dimensional space. They are suitable for any advection and diffusion problem such as: Navier Stokes equations ; Multiphase media; Gas dynamics; Vlasov-Maxwell equation.

3. THE MODEL PROBLEM

The objective is to consider an obstacle–free computational domain and in the frame work of a low order unsteady scheme we are aimed to use a vorticity– velocity– temperature particle blob approach with a Lagrangian formulation that is typically second order.

The present approach considers the analysis of the Helmholtz equations that are obtained as the curl of the momentum term of the Navier Stokes. In this formulation the pressure disappear and the velocity field is implicitly solenoidal. The problem of solenoidality that deals with the vorticity field does not arise in 2D problems that are the scope of this explorative analysis.

This approach avoid the imposition of the divergence free velocity field and of the asymptotic pressure closure condition needed for fixing mass flow in buoyant problems that is very difficult to impose and represent one of the weak points of many industrial codes.

The formulation, Golia *et al.* [22], [23], [24], [25], furthermore makes use of a splitting technique of Chorin [26], [27], that separates explicitly convective and diffuses steps, recasting the problem in a hyperbolic one for the particle and in parabolic problems for the diffusive and source phenomena that occur along each particle path.

We do not consider flows around solid body by Brinkman double penalization, Fig. (3). In this regard we shall consider 3 zones (fluid, Brinkman layer, solid body) that are defined by a time varying mask function.Then for the generic p-th particle located at r_p at time t, we must solve the following initial value problem (in case of constant diffusive properties):

Convective steps (trajectory of the p-th particle):

$$\frac{d\, r_p}{dt} = U(\underline{r}_p, t) \tag{11}$$

Diffusive Step (variations of the field properties of the p-th particle along its trajectory):

$$\frac{\partial \underline{\omega}_p}{\partial t} = \begin{cases} \dfrac{1}{Re}\nabla^2 \underline{\omega}_p - \beta\left[\underline{g} \wedge \underline{\nabla}T_p\right] & \text{fluid} \\[2em] \dfrac{1}{Re}\nabla^2 \underline{\omega}_p - \left[\dfrac{\underline{\nabla} \wedge \left(\underline{V}_p - \underline{V}_{body}\right)}{\eta}\right] & \text{Brink. Layer} \end{cases} \tag{12}$$

$$\underline{\omega}_p = \underline{\nabla} \wedge \underline{V}_{body} \qquad\qquad \text{Solid Body}$$

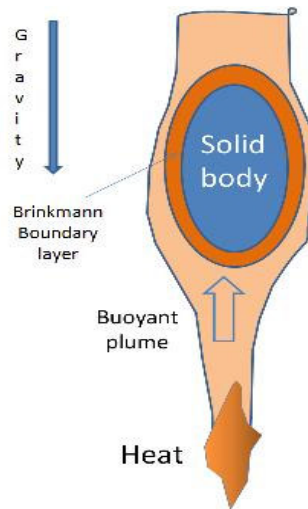$$\frac{\partial T_p}{\partial t} = \frac{1}{Re\,Pr}\nabla^2 T_p \tag{13}$$

FIGURE 3: The Brinkman Layer.

Note that:
• in the buoyant term 'β' denotes the thermal coefficient of expansion
• η <<1 is a penalization parameter
• we have not considered the dissipative term in the energy equation since it is very small and it is usually discarded in case of buoyancy.
• we do not consider buoyancy in the Brinkman Layer

- the error introduced, see [3], is expected to be of the order $\eta^{-1/4}$

The Blob representation of the eqns. (11), (12), (13) - detailed elsewhere [22], [23], [24], [25] - considers as field unknowns the p-th particle local "Vortex intensity" $\Gamma_p = \omega_p \Delta V_p$ (i.e. local velocity circulation) and the p-th particle local "Thermal intensity" $\Theta_p = T_p \Delta V_p$.

The velocity field needed in (12) is computed using an Helmholtz decomposition, i.e. as sum of a potential velocity field and a vortical velocity field computed with a generalized Biot-Savart law. This is a weak point of the Blob Vorticity Methods since the velocity of a given blob, induced by all the N vortex blobs present in the field, represents a classical N-Body problem that require $O(N^2)$ calculations. The deriving computational burden is obviously not acceptable in problems where N increase very rapidly in time. To overcome this fact, we use an "in house" Adaptive Fast Multipole Method (FMM) [28] that results to be a O(N) algorithm. The FMM was devised to be capable of self organize in order to reach optimal computation conditions while N is varying and able warrant an imposed error level on the calculation of the velocity field induced by the vortex blobs. The blob representations of the Laplacian diffusive terms and of the Gradient terms present in (12) and (13) are performed according to the Particle Strength Exchange (PSE) method proposed by Degond & Mas-Gallic [29]:

$$\nabla^2 \underline{\Gamma}_p = \sum_{q=1}^{N} \left(\underline{\Gamma}_p - \underline{\Gamma}_q \right) \mathrm{Lapl}\left(\underline{r}_p - \underline{r}_q, h \right) \tag{14}$$

$$\underline{\nabla} \, \Theta_p = \sum_{q=1}^{N} \left(\underline{r}_p - \underline{r}_q \right) \left(\Theta_p + \Theta_q \right) \mathrm{Grd}\left(\underline{r}_p - \underline{r}_q, h \right) \tag{15}$$

The kernels Lapl(•,•) and Grd(•,•) used here are the high order ones according to Eldredge et alia [30]. The PSE discretization of the differential operators are quite accurate for blobs regularly distributed in the field and away from boundaries/discontinuities. Usually, after a number of integration steps, to avoid inaccuracy due to the typical Lagrangian distortion of the particle field, a re-gridding process is performed to project the field on a regular mesh. New particles are allocated on the new mesh points and their values are interpolated from the cluster of the neighborhood ones, on the old disordered lattice, with a suitable kernel function:

$$F_p^{new} = \sum_{q=1}^{\substack{\text{Neighborhood} \\ \text{Cluster}}} F_q^{old} \, W_{regrid}\left[\left(\underline{r}_p^{new} - \underline{r}_q^{old} \right), h \right] \tag{16}$$

The kernel W_{regrid}(•,•) used here is compact over $r/h=2.5$ and is third order accurate [31].

After the discretization of each term of (11), (12), (13), it results in an initial value problem (I.V.P.) problem that requires the time integration of N-equations. This is performed, in general with a 2nd order algorithm.

It must be said that for particles located within the Brinkman Layer the problem is extremely stiff. The time integration can produce oscillations or inaccuracies if the time step "dt" is not enough smaller then the value of the penalty parameter "η". This is a burden since in order to have sufficient accuracy the penalty parameter "η" must be at least of order of 10^{-4}.

In this work we use different strategies for the time integration for particles located in particular volume phase. For fluid particle we use a 3rd order Adams-Bashforth method that computes the "n+1 time step" values using the old values at the "n time step" and at the "n-1 time step".

For particles located in the Brinkman Layer we use a first order implicit method. Future work will test various methods to improve accuracy in order to use larger values of the ratios of time steps over penalty parameters.

4. THE VALIDATION

Validations are needed to ascertain the preliminary accuracy of the original Thermal-Blob method before the use of the Double Brinkman Penalization. In the following we shall present various tests that consecutively validate each particular segments of the method and of the relative code.

4.1 Inviscid elliptical vortex blob patches

Scope of this test is to validate the accuracy of the routines for computation of the velocity field induced by the vortex blobs and for the time integration of the blob's particle paths.

We do consider a classical inviscid Elliptical Vortex Blob Patches (Lambs' vortex) that [32] will rotate steadily and as rigid body, according to the value of the (constant) patch vorticity and to the values of the semi axes a, b, with the angular velocity:

$$\Omega_{rot} = \omega_{patch} \frac{ab}{(a+b)^2} \tag{17}$$

The time frames depicted in Fig. 4 show the almost perfect rigid body rotation (no regrinds), thus validating the computation of the induced velocity and of the time integration routines.
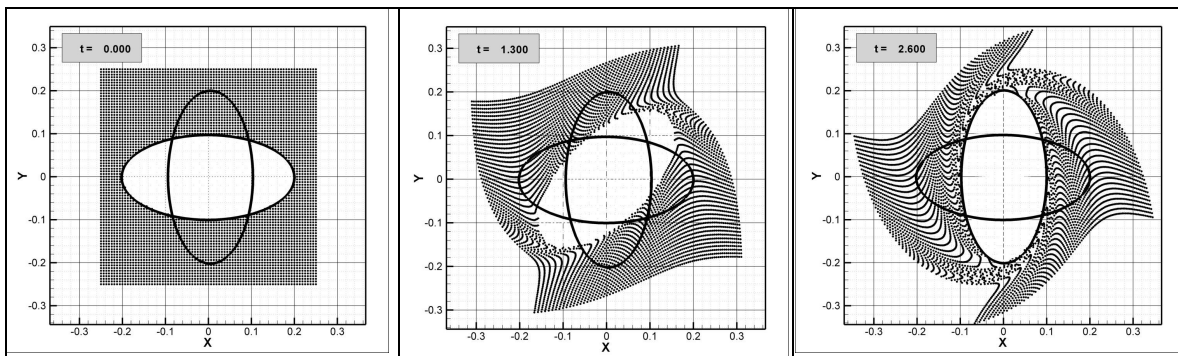

FIGURE 4: Inviscid Elliptic Patch at Various Times.
Nx=Ny=81; dx=dy=0.00625; dt=0.00125, $\omega_{patch} = \pi$, Vel. Acc.= 10^{-4}

4.2 Free buoyant thermal blob patches

Scope of this test is the validation of the routines that compute Laplacian (diffusion processes) and gradients, the correctness of the buoyant term and the effectiveness of the regrid processes.

We consider an initially Thermal Free Patch in a gravity field undergoing buoyant and diffusion processes. The patch rising will split in two anti rotating cores due to the vorticity created by the buoyancy term in eqn.(12). Geometrical symmetry is expected and global vorticity must be conserved to zero.

Fig. 5 represents the real computational field and the evolution of the blobs particles, colored according to their temperature. It is interesting to note as the Lagrangian formulation allows the code to be completely adaptively and grid free. The blobs naturally go where needed and the code automatically creates new particles according to the vorticity generations.

The run corresponds to the following parameters: Gr=0.65107; Pr=0.748; h=0.01; dt=0.0125. At t=0, the initial, number of blobs is 2511 and grows spontaneously up to 8919 , at t=5.
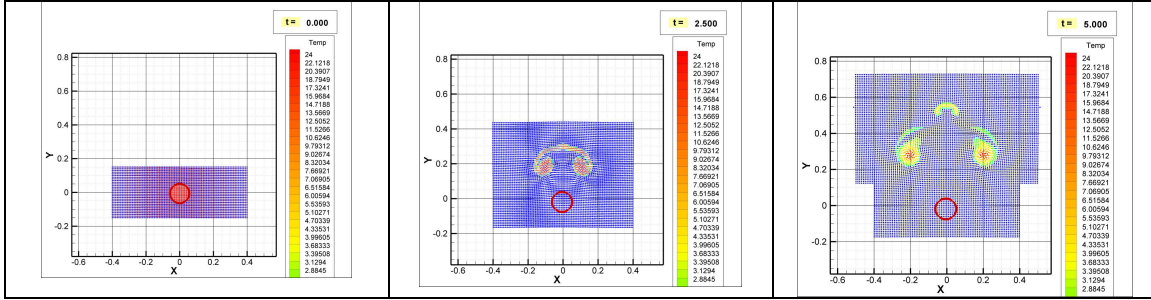
FIGURE 5: Free Plume Convection of Thermal Free Patch Initially Circular.

4.3 Free buoyant thermal-vortex blob patches

Scope of this test is the validation of the coupling of the thermal buoyant process with the dynamics effects of a non zero initial vortex patch. Here we consider an initially circular Free Patch of blob particles, having both Thermal and Vortex content, placed in a gravity field, that undergoes buoyant and diffusion processes.

Due to the vorticity created by the buoyancy term in (12), the rising patch will split in two anti rotating cores. But in this case geometrical symmetry is not maintained due to the fact that global vorticity must be conserved to the non zero initial value.
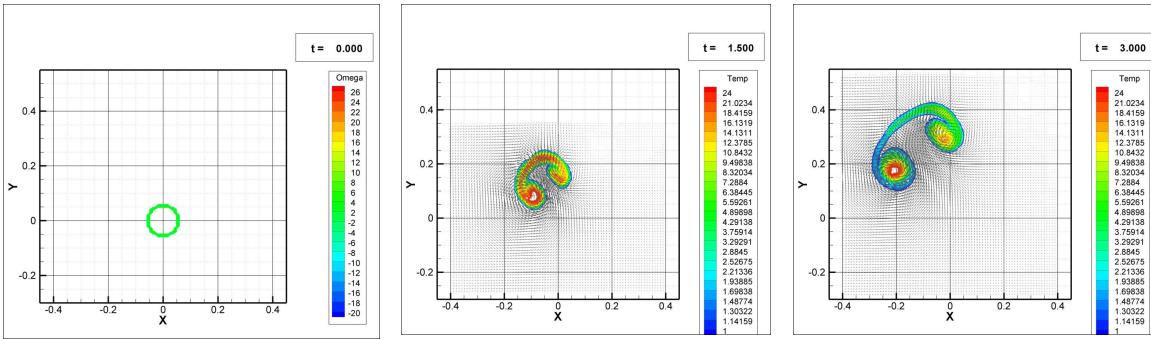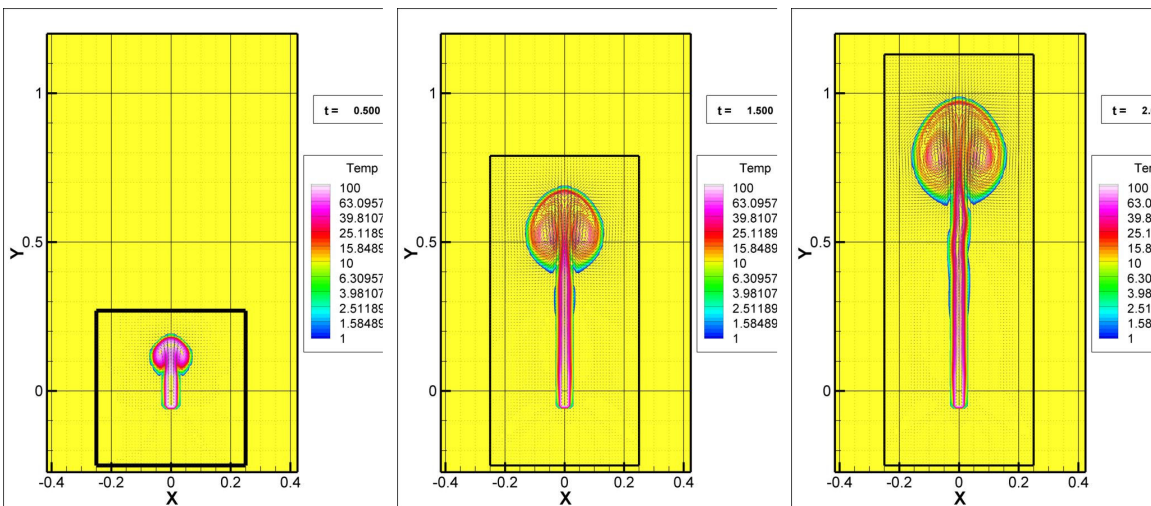

FIGURE 6 : Free Plume Convection of Vortex-Thermal Free Patch Initially Circular.
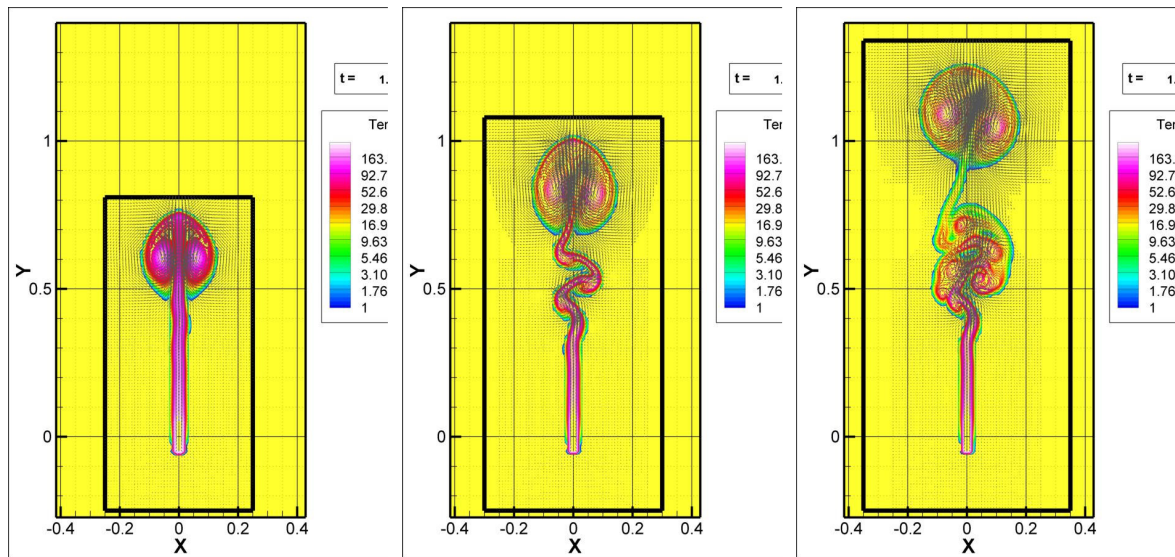
FIGURE 7: Free Buoyant Rising Plume from a Thermal Blob Patch at Different Grashof Numbers.

As shown in [33], integral balance laws impose according to the sign of the initial vorticity, that one of the two cores rotates more (i.e. will have larger vorticity) than the other.

Fig. 6 reports the evolution of the iso-vorticity contours. The computational parameters are: Pr=0.748; h=0.1, dt = 0.00125, V_{ref}=0.125 10-3; L_{ref} = 0.1188, Rey=1, regrid process is performed after 10 time steps.

It is interesting to note that, as predicted, the initial circular blob path rising is split in two counter-rotating ones, the left one having a large vorticity content of the other, then having higher angular rotation velocity. Since, the global of vorticity content must be constant as the initial one, the rotation difference of the two cores will vary in time. Therefore the iso-vorticity contours undergo higher relative changes with respect to the thermal ones.

4.4 Fixed buoyant thermal blob patch

Scope of the test is to verify the free buoyant rising plume that stems from a Thermal Blob Patch which is maintained fixed and at a constant temperature. The same Patch will be hereafter considered to generate a thermal plume that shall interact with solid bodies (still or moving).

Fig.7 reports the thermal contours of the rising plume at various times, for different Grashof numbers: the top row refers to Gr=0.25 10^8, the bottom row refers to Gr=0.625 10^8. Temperature level refers to temperature rise with respect to the asymptotic one. Both case are relative to an elliptical fixed thermal patch having a=0.0198 and b=3a. The run corresponds to the following parameters: Gr = 0.65 10^7 ; $Rey_{\Omega D}$ = 0.243 10^4 ; Pr = 0.748 ; h = 0.01 ; Δt = 0.0125. The initial (at t=0) number of blobs is 41311, and grows spontaneously up to 67220, at t=3,.

Even if the value of the reference blob distance "h" is not small enough to reach turbulent scale, it is evident, from the figure, the capacity of the method and of the code to catch the instability of the rising plume that is verified at a certain rising distance from the standing thermal patch.

5. PLUME-BODY INTERACTIONS

In this paragraph we consider the interaction of the thermal buoyant plume (described in the previous paragraph) with a body using the Brinkman Layer as per Fig. 3. In the following, we shall present the interactions of the rising plume with a still blunt body, with a still slender body and with a slender moving body (linear motion and rotation).

5.1 Plume interaction with a still blunt body

The data of the thermal plume are as the ones of the top row of Fig. 7.

The body is an ellipse b/a=3 staying still above a thermal patch that originate a buoyant plume. The body is at zero temperature rise and the Brinkman layer has a thickness twice the blob nominal distance "h".

Fig. 8 shows three frames of a video clip referring to the touching of the plume mushroom with the Brinkman Layer of the body and two other significant later states, namely the breaking of the mushroom and the lateral migration of the two counter-rotating vortices generated by the interaction.
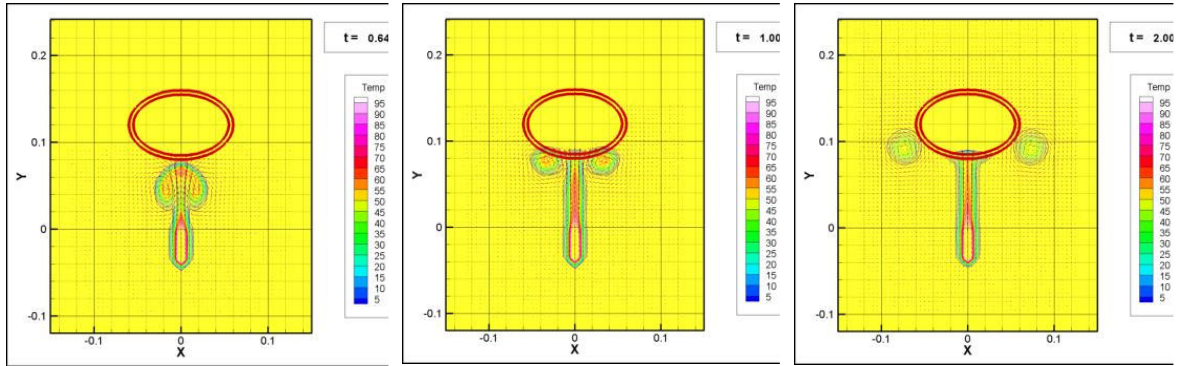

FIGURE 8: Plume Interaction with a Still Blunt Body Simulated with Brinkman Layer.

5.2 Plume interaction with a still slender body

The same comments as the ones of paragraph 5.1 apply, but here the elliptical body, as depicted in Fig. 9, is rotated by 90° normally to the gravity vector to represent a slender obstacle for the rising plume. In this case a quite lighter interaction is expected and the migration of the two counter-rotating vortices generated by the interaction is quite faster. The technique used to highlight the temperature contours emphasizes the automatic dynamic development of the computation field that, at the initial stages, does not contain the body.
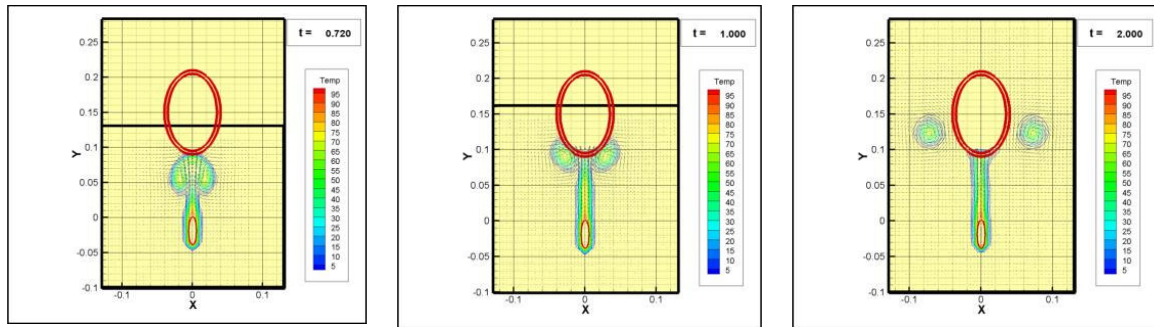

FIGURE 9: Plume Interaction with a Still Slender Body Simulated with Brinkman Layer.

5.3 Plume interaction with a transverse moving body

The data of the thermal plume are as the ones of the top row of Fig. 7. The body is an ellipse with b/a=3, oscillating horizontally (normally to the gravity vector) with an amplitude of 0.2 and a period of 0.82. The body is at zero temperature rise and the Brinkman layer has a thickness twice the blob nominal distance "h".

The images in Fig. 10 report the blobs position and the velocity vector. In the top row the blobs are colored according to the local vorticity, in the bottom row the blobs are colored according the local temperature rise.

As a check, the invariance of the zero total vorticity over a full period of oscillation is verified. The oscillatory motion of the solid body is synchronized such that at time t=1 the plume top mushroom hits the bottom of the body.
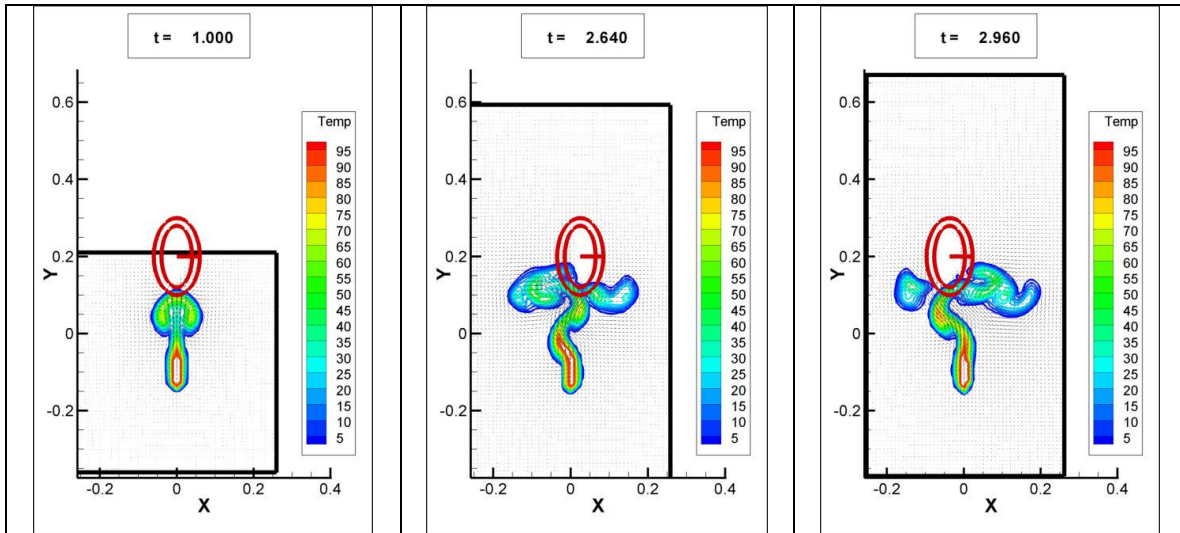

FIGURE 10: Thermal Plume Interacting with a Slender Body Oscillating Laterally (contours).
Figure 10 reports some shots that reveal the strike and the relative hysteresis phenomena of the flow pattern. The t = 2.64 shot refers to the ellipse moving west ward, the t = 2.96 shot refers to the ellipse moving eastwards. Obviously the running of the video clip can better reveal the dynamics of the interaction and the realistic behaviors of such a complicate unsteady interaction.
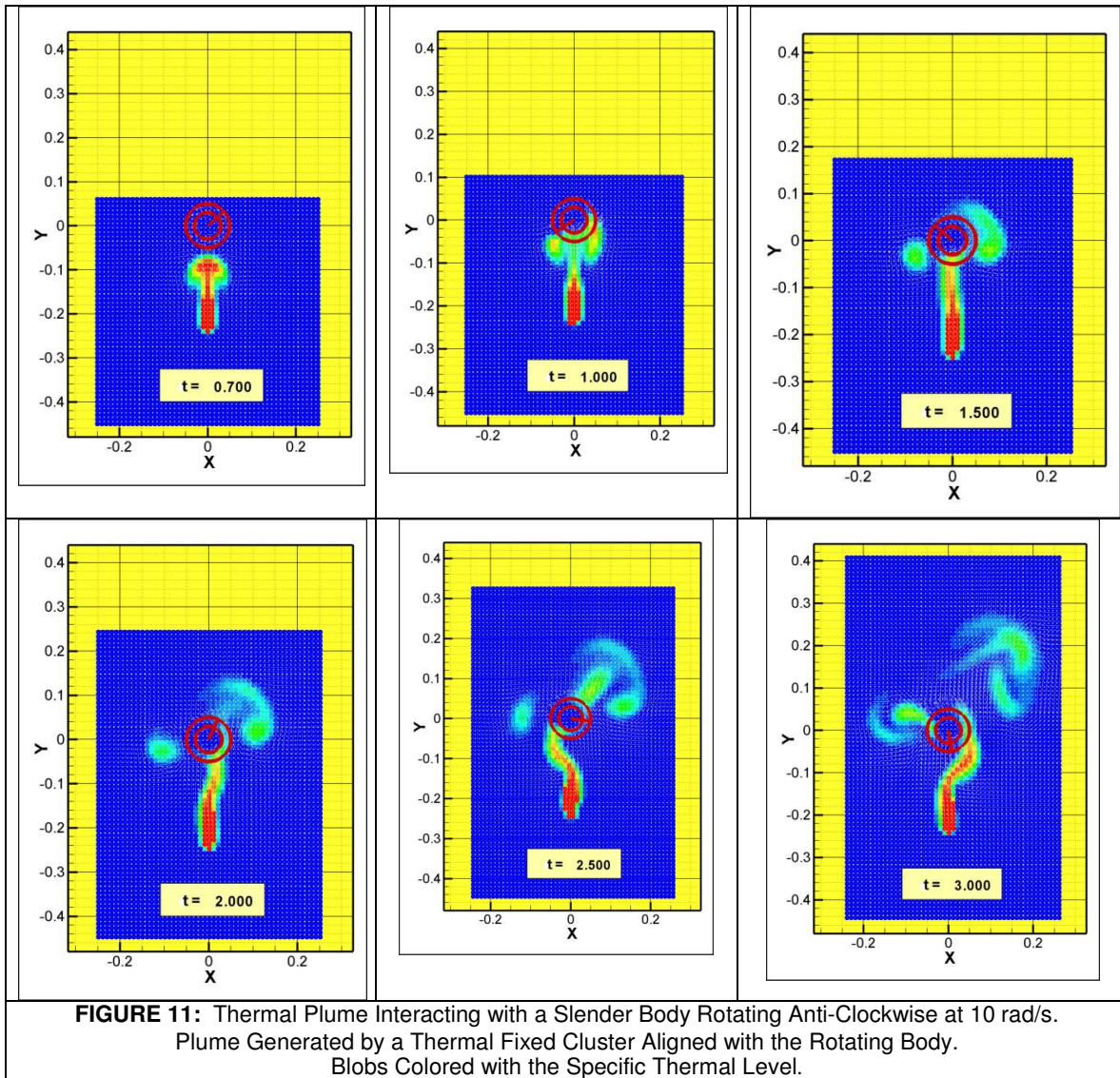
5.4 Plume interaction with a rotating body
In this case we consider a thermal plume generated by a thermal fixed particle cluster posed below a circular body that rotates with a given angular speed Ω_b anti-clockwise.
Fig.11 refers to the case Ω_b= 10 [rad/s] with hot blob cluster aligned below the rotating body.
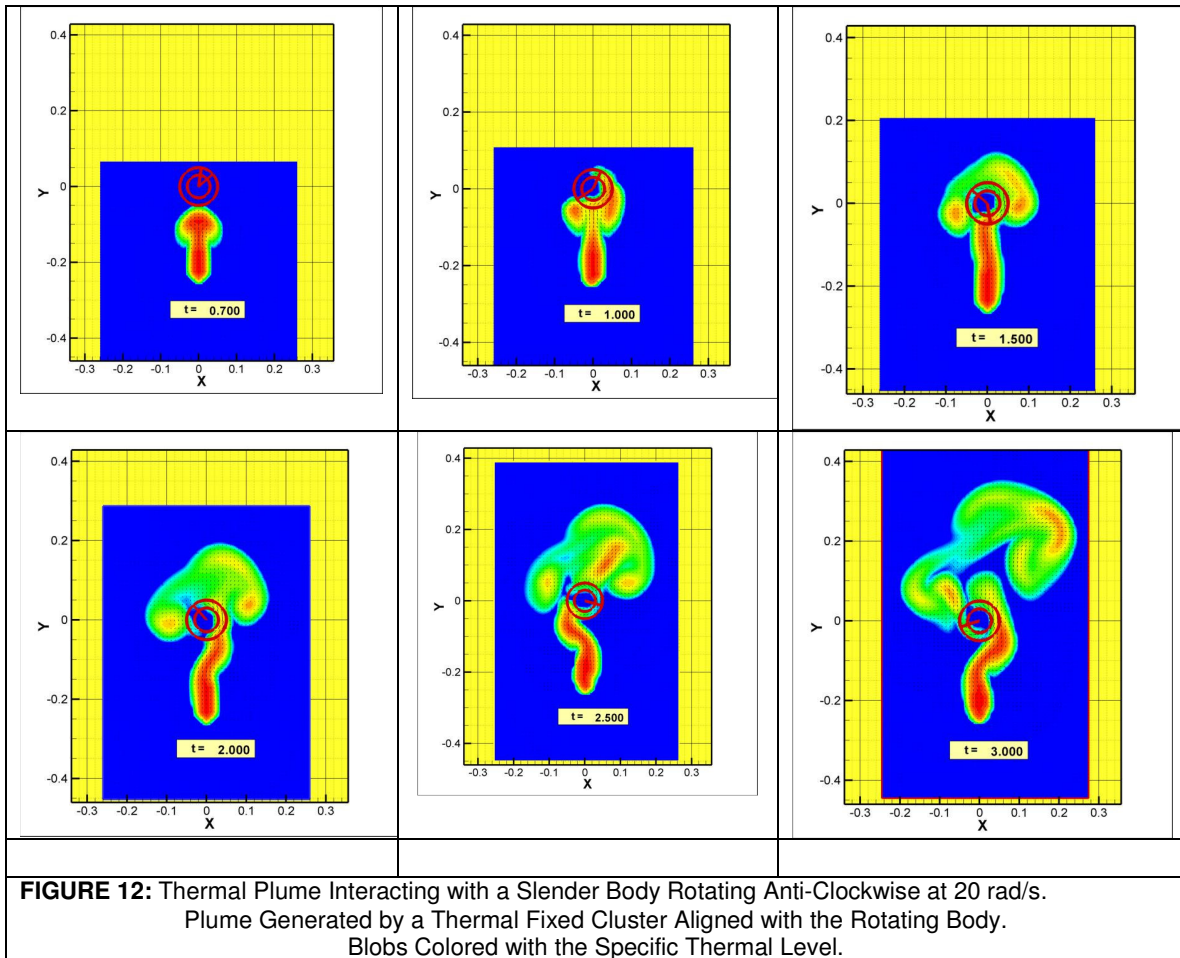Fig.12 refers to the case Ω_b= 20 [rad/s] with hot blob cluster aligned below the rotating body.
Fig.13 refers to the case Ω_b= 30 [rad/s] with hot blob cluster misaligned below the rotating body.
The six shots of each Figure refer to different times and display blobs colored according the specific temperature value. We can notice:

FIGURE 11: Thermal Plume Interacting with a Slender Body Rotating Anti-Clockwise at 10 rad/s. Plume Generated by a Thermal Fixed Cluster Aligned with the Rotating Body. Blobs Colored with the Specific Thermal Level.

- the capacity of the approach to generate automatically blobs, as needed, that moves in the region where thermal and vorticity effects are relevant.
- the different dynamic behavior of the plume:
  - In the initial stage the steam of the plume is linked with the mushroom cap that contains anti-rotating vortical structures: the sting furnish energy to the cup enough to overcame the loss of thermal and kinetic energy due to heat conduction and to viscous effects: it derives a certain stability for the sting;
  - In the latter stage a pinch-off phenomena is verified: the sting separates for the cup that is no longer feden;
  - It derive that the cup tends to decrease the rotation speed and to fragmentize whereas the sting loses it stability and oscillates laterally (as a candle) due, from one side, to the rotation of the top body and from the other side, to the need to obey to conservation of its global vorticity;
  - This is evident in the last shots of all figures, but in particular in Fig. 13 where the sting is first moved away by the anti-clockwise rotation of the body and after is attracted.

FIGURE 12: Thermal Plume Interacting with a Slender Body Rotating Anti-Clockwise at 20 rad/s.
Plume Generated by a Thermal Fixed Cluster Aligned with the Rotating Body.
Blobs Colored with the Specific Thermal Level.

6. CONCLUSIONS & FUTURE WORK

The use of the Brinkman penalization method to simulate the layer over a body considered as a porous media appears compatible with the grid free Lagrangian Vortex and Thermal Method developed by the authors. This method seems quite sound for simulating the viscous interaction of plumes and bodies since is based on fluid dynamics considerations that confine diffusive phenomena in segregated regions near the body.
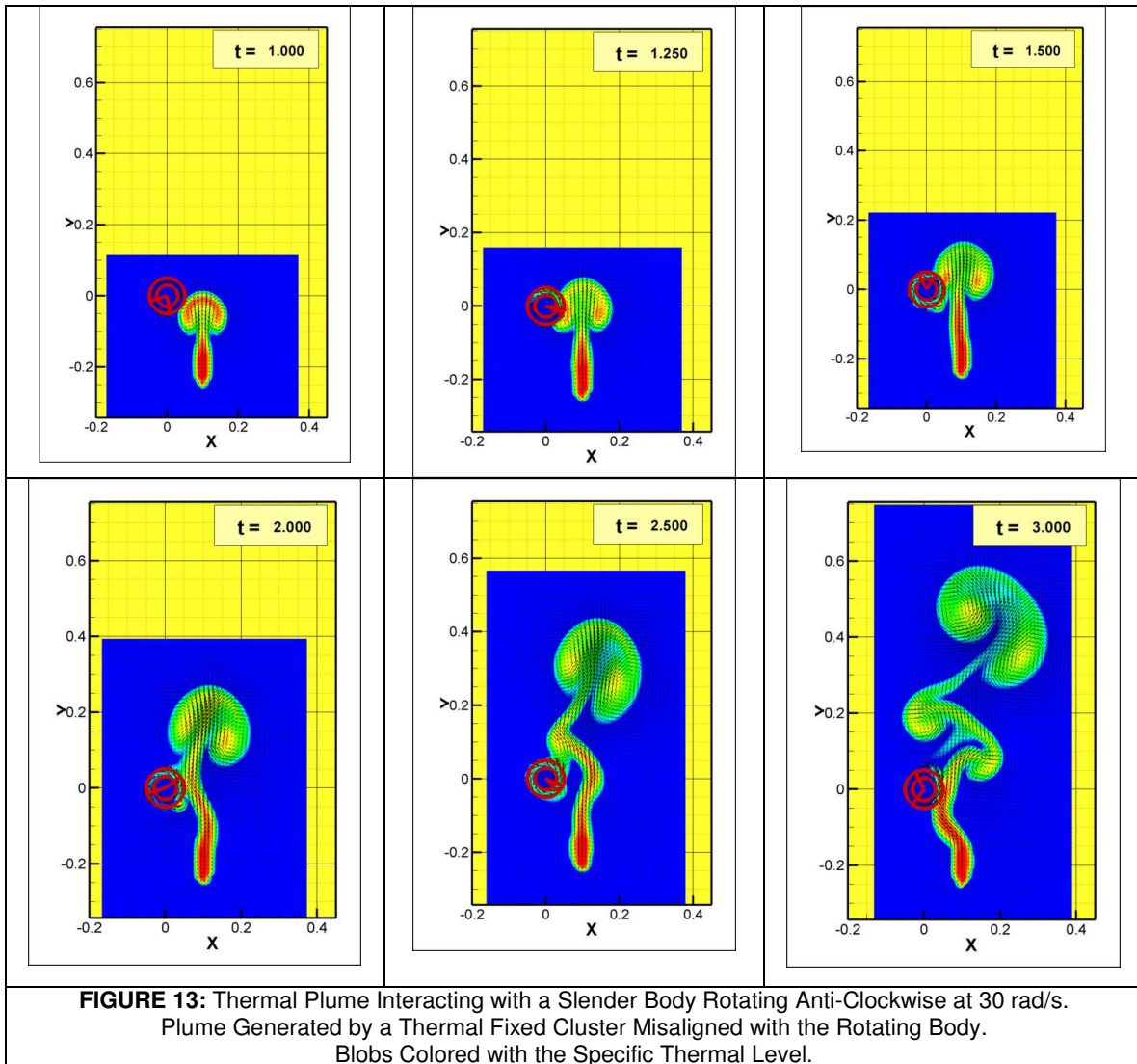
The first experience is positive but further works are required mainly in relation to the time integration of the diffusion processes for particles within the Brinkman Layer. The use of implicit scheme was experienced to be necessary, but further analysis is recommended in order to optimize peculiar schemes to improve the ratio of the time step interval over the penalization parameter. It must be underlined that dealing with unsteady motion of the body was quite simple and the relative effort limited mainly to the development of an efficient masking procedure, and to the of the time integration step that must be small enough with respect to the oscillation period.

In this preliminary analysis we did not consider the thermal interaction between the plume and the thermal characteristics of the body (considered at zero temperature rise). This is a quite large field of analysis that comprise, among other, all the various thermal conditions on the body, and the insertion of heat flux within the body itself and others.

It is obvious that further work should be reserved also to forced and mixed thermal convection and to real porous bodies. The working agenda is certainly quite full.

We do want to conclude this paper by stating that the first experience is definitely positive since the mix of the adaptive Lagrangian Blobs method with Brinkman penalization generates a

computational environment quite handy and efficient for the analysis of quite complicated problems of real interest in engineering science.

FIGURE 13: Thermal Plume Interacting with a Slender Body Rotating Anti-Clockwise at 30 rad/s. Plume Generated by a Thermal Fixed Cluster Misaligned with the Rotating Body. Blobs Colored with the Specific Thermal Level.

7. REFERENCES

1. Arquis,E. , Caltagirone,J-P., Vincent,S. "*Sur le conditions hydrodynamique au voisinage d'une interface millieux fluid-millieux poreux: application à la convection naturelle*". C.R. Acad. Sci. Paris, Series IIb, 299: 1-4, 1984
2. Angot, Ph.. "*A Mathematical and numerical modelling for a fictious domain method with penalized immersed boundary conditions*". HDR thesis, Universitè Mediterranée, Aix-Marseille,1998
3. Angot, Ph., Bruneau C.H., Fabrie, P.. "*A penalization method to take into account obstacles in incompressible viscous flows*". Numerische Mathematik, 81(4): 497-520, 1999
4. Caltagirone,J-P., Vincent,S : Sur une methode de penalisation tensorielle pour la resolution des equations de Navier-Stokes, C.R. Acad. Sci. Paris, Series IIb, 329: 607-613, 2001
5. Khadra, K., Angot,Ph., Parneix, S., Caltagirone,J-P.. "*Fictitious domain approach for the numerical modeling of Navier-Stokes equations*". Int. J. Numer. Methods in Fluids, 34 (8): 651-684, 2000

6. Schneider,K. ,Farge, M. .”Coherent Vortex Simulation (CVS) of a 2D bluff body flow using an adaptive wavelet method with penalization”. Advances in Turbulence, 9: 471-474, 2002
7. Schneider, K. ,Farge, M. “Adaptive Wavelet Simulation of a flow around an impulsively started cylinder using penalization”. Applied and Computational Harmonic Analysis, 12: 374-380, 2002
8. Schneider,K. ,Farge, M. ”Numerical simulation of dipole-wall interaction using an adaptive wavelet discretizatuion with volume penalization”. ENUMATH (eds. Bermudiz et alia), Springer, 822-830 (2005)
9. Schneider,K. ,Farge, M. ”Numerical simulation of transient flow behaviour in tube bundles using volume penalisation method”. Journal of Fluids and Structures, 20 (4): 555-566, 2005
10. Schneider,K. “Numerical simulation of the transient flow behaviour in chemical reactors using penalization method”. Computers and Fluids, 34(10): 1223-1238, 2005
11. Vasilyev,O.V , Kevlahan, N.K.R. “Hybrid wavelet collocation-Brinkman penalization method for complex geometry flow”. Int. J. Numer. Methods in Fluids, 40(3-4): 531-538, 2002
12. Kevlahan, N.K.R., Vasilyev,O.V., Goldstein, D., Jay, A. “A adaptive wavelet collocation method for fluid-structure interaction at high Reynolds number”. SIAM J. Sci. Comp., 26 (6): 1894-1915, 2005
13. Kevlahan, N.K.R., Ghidaglia JM. “Computation of turbulent flow past array of cylinders using spectral method with Brinkman penalization”. Eur. J. Mech. B - Fluids, 20:333-350, 2001
14. Bruneau,C.H. , Mortazavi I. “Control of Vortex Shedding Around a Pipe section Using a Porous Shealth”. International Journal of Offshore and Polar Engineering, 16: 90-96, 2006
15. Chiavassa G. , Donat R. “Point Value Multiscale Algorithms for 2D Compressible Flow”. SIAM J. Sci. Comp., 23 (3) : 805-823, 2001
16. Bruneau,C.H. , Mortazavi I. “Controle passif d'ecoulement autour d'obstacles par les milieux poreaux”. C.R. Acad. Sci. Paris, Series IIb, 329 :517-521, 2001
17. Bruneau,C.H. , Mortazavi I. “Passive control of the flow around a square cylinder using porous media”. Int. J. Numer. Methods in Fluids, 45(4): 415-433, 2004
18. Carbou,G. , Fabrie P “Boundary Layer for a penalization method for viscous compressible flow”. Adv. Differential Equations, 8 :1453-1461, 2003
19. Carbou,G. “Penalization method for viscous incompressible flow around a porous thin layer”. Nonlinear Anal. Appl., 5: 815-855, 2004
20. Carbou,G. “Brinkman Model and Double Penalization Method for the Flow around a Porous Thin Layer”. J. Math. Fluid. Mech., 10: 126-158, 2008
21. Cottet,G.H. and Koumoutsakos,P.D. “Vortex Methods: Theory and Practice”. Cambridge University Press, 2000
22. Golia,C., Buonomo,B., Manca,O., Viviani, A. “A Vortex-Thermal Blobs Method For Unsteady Buoyancy Driven Flows”. ASME-IMECE, Anaheim (CA), 2004, Paper IMECE-2004-59180
23. Golia,C., and Buonomo,B. “An Effective Blob Approach to Unsteady Thermal Buoyant Flow”. CMEM, Malta, 2005
24. Golia,C., and Buonomo,B. “Numerical Simulation of Unsteady Natural Convection by Blobs Methods”. 60th ATI Congress, Roma, 2005
25. Golia,C. and Buonuomo,B. “On the accuracy of integral representation of differential operators in meshless Lagrangian blob method”. CMEM, Praga, 2007.
26. Chorin, A.J. “Numerical Study of Slightly Viscous Flow”. Journal of Fluid Mechanics 57 (4) : 785-796, 1973
27. Chorin, A.J. “Vortex sheet approximation”. J. Comp. Phys., 27 (3) : 428-442, 1978
28. Greengard L., Rokhlin, V. “A fast algorithm for particle simulation”. J. Comp. Phys., 73 (2): 325-348, 1987
29. Degond,P. and Mas-Gallic,S. “The weighted Particle method for Convection-Diffusion Equations, part.1: the case of an isotropic viscosity”. Math.s of Computation, 58 (188) : 485-507, 1989
30. Eldredge,J.D., Leonard,A. and Colonius,T. “A General Deterministic Treatment of Derivatives in Particle Methods”. J. Comp. Phys., 180 (2): 686-709, 2002
31. Meijering, E., Unser, M. “A Note on Cubic Convolution Interpolation”. IEEE Trans. Image Process, 12 (4): 477-479, 2003
32. Batchelor G.K. “An Introduction to Fluid Dynamics”. Cambridge Univ. Press, 1967

C. Golia, B. Buonomo & A. Viviani

33. Riccardi G., Golia C. *"Integral Balance Laws for 2D buoyancy driven flows".* VII SIMAI Congress, Venice, 2004.